Journal of Magnetism and Magnetic Materials 474 (2019) 493–500

Contents lists available at ScienceDirect

Journal of Magnetism and Magnetic Materials

journal homepage: www.elsevier.com/locate/jmmm

Research articles

Effect of magnetic frustrations on magnetism of the Fe_3BO_5 and Co_3BO_5 ludwigites

Yu.V. Knyazev[a], N.V. Kazak[a,*], I.I. Nazarenko[a], S.N. Sofronova[a], N.D. Rostovtsev[b], J. Bartolome[c], A. Arauzo[d], S.G. Ovchinnikov[a]

[a] Kirensky Institute of Physics, Federal Research Center KSC SB RAS, 660036 Krasnoyarsk, Russia
[b] Siberian State University of Science and Technologies, 660014 Krasnoyarsk, Russia
[c] Instituto de Ciencia de Materiales de Aragón, CSIC-Universidad de Zaragoza and Departamento de Física de la Materia Condensada, 50009 Zaragoza, Spain
[d] Servicio de Medidas Físicas, Universidad de Zaragoza, Pedro Cerbuna 12, 50009 Zaragoza, Spain

ARTICLE INFO

Keywords:
Antiferromagnetics
Superexchange interactions
Frustrations

ABSTRACT

The magnetic structures of Fe_3BO_5 and Co_3BO_5 ludwigites have been studied experimentally by magnetic measurements and theoretically by the combination of the group theoretical analysis and semi empiric calculations of the superexchange interactions. The different collinear spin configurations in the triads 3-1-3 and 4-2-4 including ferromagnetic, antiferromagnetic and dimer have been considered. For Fe_3BO_5 the antiferromagnetic state with zero magnetic moment per unit cell, showing the lowest energy, results to be the most probable magnetic ground state. The unusual magnetic structure comprising two virtually independent orthogonal subsystems is formed to avoid heavy frustrations of superexchange interactions between the 3-1-3 and 4-2-4 spin ladders. In Co_3BO_5 the magnetic frustrations present for the Co^{3+} high-spin state are quenched for a Co^{3+} low spin state resulting in the ferrimagnetic long-range order. The obtained results are discussed in comparison with experimental magnetic data.

1. Introduction

Low-dimensionality and frustrated magnetism are two topics in condensed matter physics that are currently under intense investigation. These phenomena play a fundamental role in establishing a magnetic ground state leading to exotic states such as spin liquid, spin ice, and noncollinear magnetic structures [1–3]. The oxyborates with ludwigite structure are antiferromagnets which structure contains triangular magnetic arrangements, where geometric frustrations are expected to exist [4]. In the past two decades, the investigations on ludwigites have been focused on atomic instability, low-dimensional crystalinity, and often puzzling magnetic structures [5–10].

The ludwigites with general formula $M_2^{2+}M^{3+}BO_5$ (M^{2+}, M^{3+} = Mg, or 3*d* metal) crystallize in orthorhombic symmetry (*Pbam*) with metal ions occupying four crystallographically inequivalent sites 1, 2, 3, and 4 inside of oxygen octahedra (Fig. 1). The trivalent ion predominantly occupies the site 4, while divalent ions occupy 1, 2, and 3 metal sites. The triads 4-2-4 and 3-1-3 with shortest and longest interionic distances are structurally singled out. The triads are linked in quasi-one-dimensional magnetic substructures – three-leg spin ladders (3LL) propagate along the *c*-axis. The ludwigites can be formed with most of the transition metals, allowing the variation of basic parameters of spin, charge, and orbital subsystems [9,11,12].

Up to date there are only two known homometallic ludwigites Fe_3BO_5 and Co_3BO_5 which show quite different structural, magnetic and electronic properties [7,13]. The Fe_3BO_5 undergoes a structural orthorhombic – orthorhombic transition at T_{ST} = 283 K (*Pbam* No.55 – *Pbnm* No.62), which is accompanied by small atomic displacement of Fe2 ion in the 4-2-4 triad and the duplication of the *c* axis [6,8]. A cascade of magnetic transformations takes place with temperature decrease: PM-AFM1-F-AFM2 as found from the Mossbauer Effect (ME) [8], heat capacity [10] and magnetization studies [14]. The antiferromagnetic ordering of Fe2 and Fe4 (AFM1) magnetic moments appears at T_{N1} = 110 K. The ferrimagnetic (F) ordering involves the Fe1 and Fe3 magnetic moments at T_{N2} = 74 K. The 3D antiferromagnetic order (AFM2) is assumed to set on below T_{N3} = 30 K [8,14]. A temperature-induced change of the anisotropy axis from *a* to *b*-axis in the low-temperature antiferromagnetic phase was found in Fe_3BO_5. In contrast, Co_3BO_5 has a more conventional behavior, with a ferrimagnetic transition at T_N = 42 K and no structural transformations [10,13,14]. Moreover, at all temperatures below T_N a high magnetic uniaxial anisotropy (*b* axis) has been observed.

* Corresponding author.
E-mail address: nat@iph.krasn.ru (N.V. Kazak).

https://doi.org/10.1016/j.jmmm.2018.10.126
Received 28 June 2018; Received in revised form 11 October 2018; Accepted 26 October 2018
Available online 27 October 2018

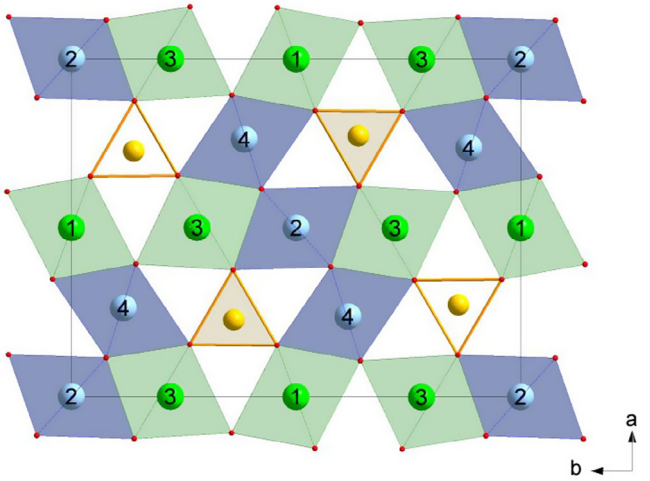

Fig. 1. Ludwigite crystal structure (sp.gr. Pbam (55)) projected along the *c*-axis. The four different crystallographic sites occupied by metals are numbered. The triangle BO_3-group are shown. The triads 3-1-3 and 4-2-4 are indicated by green and blue, respectively. (For interpretation of the references to colour in this figure legend, the reader is referred to the web version of this article.)

The accurate description of the Fe_3BO_5 magnetic structure is a subject of extensive studies both experimental and theoretical. Neutron powder diffraction (NPD) measurements were performed at 5 [4], 10 and 82 K [15]. The investigations have shown that two magnetic subsystems 4-2-4 and 3-1-3 are ordered independently and orthogonally: at T_{N1} the 4-2-4 spin ladder is antiferromagnetically ordered with all magnetic moments being aligned along *b*-axis with zero magnetic moment per unit cell. According to Bordet et al. [15], the spin arrangement along the triad 4-2-4 is ferromagnetic (↑↑↑) with AF coupling between them along *c*-axis. As a result, the ferromagnetically coupled antiferromagnetic chains extended along *c*-axis appear. Attfield et al. [4] proposed the antiferromagnetic spin arrangement (↑↓↑) along the 4-2-4 with antiferromagnetically coupled antiferromagnetic chains along the *c*-axis. The antiferromagnetic arrangement (↑↓↑) in the spin-ladder 3-1-3, leading to the antiferromagnetically coupled ferromagnetic chains running along *c*-axis with magnetic moments being aligned along the *a*-axis was found in both studies. So, according to the NPD data, the ground magnetic state of Fe_3BO_5 is a ferrimagnet with the rather large net magnetic moment ($\sim 2.36\ \mu_B$/f.u.) [15]. At the same time the diminishing of hysteresis loops below 40 K and considerably small magnetic moment, observed from the magnetization [14] and ME measurements [8], clearly indicates the transition to the antiferromagnetic state (AFM2). Inelastic neutron scattering studies could clarify the orientation of the magnetic moments in the triads 4-2-4, however, they have not yet been carried out.

Considerable efforts toward the understanding of the magnetic structure of Fe_3BO_5 have been done using different theoretical approaches. The effect of oxygen octahedral distortions on the opening of a gap at the Fermi level and the spin exchange were investigated using an extended Huckel high-spin band approach (EHTB) [16,17]. It was shown that the nearest-neighbor Fe spins in the 3LL subunits are coupled antiferromagnetically. The spin interactions between the ladders are considerably weaker than those within the ladders. The general predictions of spin arrangement in 4-2-4 and phase diagrams relating the hopping parameter *t* and spin exchange parameter *J* have been built using a tight binding Hamiltonian which includes double and superexchange terms [18]. Antiferromagnetically ordered ferromagnetic rungs and a zigzag canted spin ordering along the *c*-axis were predicted. The dimerized phase involving the Fe spins of the 4-2-4 ladder was proposed as a ground magnetic state using a density functional approach [19]. The formation of Fe^{2+}-Fe^{3+} dimers as strongly coupled magnetic units, and non-collinear spin ordering of the trivalent Fe^{3+} spin relative to the spin orientation of the dimer were considered in order to explain the low net magnetization.

To the best of our knowledge, only two works have been published so far reporting theoretical studies on Co_3BO_5. Using the EHTB method, differences in the local octahedral geometry at different sites which lead to significant differences in the charge distribution of the two homometallic ludwigites Fe_3BO_5 and Co_3BO_5, have been found [20]. The structural and electronic conditions for charge localization were obtained in Co_3BO_5. In Reference [21] an estimation of the superexchange inteactions has been made and frustration effects have been rationalized. Recently Freitas et al. [22] have found by neutron diffraction method that at low temperature (below $T_N = 42$ K) the Co^{3+} ions located at the site 4 are in low-spin state (S = 0). This is argued to be a reason for the drastic differences in the magnetism and electronic properties of the two homometallic ludwigites.

Despite numerous studies, the experimental results on Fe_3BO_5 are contradicting and several important questions remain unsolved. 1) What factor causes the separation of two quasi-low-dimensional magnetic subsystems from the three-dimensional net of the magnetic interactions in Fe_3BO_5. 2) What is the reason for the orthogonal spin ordering of these subsystems. 3) How to explain the contradiction between the small experimental magnetic moment at AFM2 phase and that expected from ferrimagnetism arising from the 3-1-3 spin ladder in Fe_3BO_5. As for Co_3BO_5, the calculation of superexchange interactions are required to clarify the effect of the Co^{3+} low spin state on the magnetic ground state of Co_3BO_5. To try to answer these questions, we have carried out the analysis of the magnetic structures of Fe_3BO_5 and Co_3BO_5 by means of a combination of group-theory analysis and semi empirical superexchange interaction calculation. We have considered different possible collinear spin configurations and found the most probable magnetic ground states in Fe_3BO_5 and Co_3BO_5.

Our study shows the crucial role of frustration in the magnetic state of Fe_3BO_5 and Co_3BO_5. We have found that in Fe_3BO_5 the antiferromagnetic superexchange interactions between 3-1-3 and 4-2-4 spin ladders are frustrated due to triangle arrangement of iron ions. In order to avoid heavy frustration, the magnetic system is split into two quasi-1D magnetic subsystems. Thus, the experimentally observed decoupling of the magnetic subsystems arises from the orthogonal spin arrangement of iron ions. The long-range order within each subsystem sets on at a relatively high critical temperature. The small value of the residual magnetic moment arises from antiferromagnetic coupling between adjacent 3-1-3 and 3′-1′-3′ spin ladders.

In Co_3BO_5 the frustrations of exchange interactions occurring for the Co^{3+} high-spin state are removed in the presence of a low spin, resulting in long-range ferrimagnetic ordering. The obtained results are discussed in comparison with experimental magnetic data for Fe_3BO_5 and Co_3BO_5.

2. Expermental techniques and computation details

The X-ray diffraction measurements were performed for Co_3BO_5 single crystal with a SMART APEX II difractometer [21].

For the magnetic structure analysis, the magnetic representation, expansion in irreducible representations and the eigenvectors that define the direction of the magnetic moments were obtained. The used method of group-theoretical analysis is described in the Supplementary Material (SM).

To assess the exchange interaction, we used the model of indirect interaction, which is developed in [23–26]. The nearest neighbours approach is used in the framework of the given model, i.e. the interaction of two 3*d*-cations through an intermediate ligand M-O-M (superexchange, SE). The strength and sign of the pair spin interactions depend on the atomic arrangement of the magnetic ions and are qualitatively predicted by the Goodenough-Kanamori-Anderson rule [27–29]. The next-nearest neighbors' interactions M-O-B-O-M and M-O-M-O-M (super-superexchange, SSE) are not considered. As a basis, the

model uses the parameters of electron transfer along the σ and π bonds, b and c, respectively, the intra-atomic exchange integral J (Hund energy) and the cation-ligand excitation energy Δ_{pd}. All five-3d orbitals of neighboring cations (α, β) and intermediate ligand three 2p-orbitals (γ) are taken into account. The sum of the individual orbital exchange integrals is a total integral of cation-cation exchange interactions in this model of the cation-ligand-cation complex:

$$J_{ij} = \frac{1}{4S_iS_j}\sum_{\alpha,\beta=1}^{5}\sum_{\gamma=1}^{3} I_{ij}^{\alpha,\beta,\gamma} \quad (1)$$

S_i, S_j are interacting cations spins, $I_{ij}^{\alpha,\beta,\gamma}$ – Superexchange integral for the i and j neighboring cations individual orbitals.

In the calculations, the X-ray diffraction data for Fe_3BO_5 [15] and Co_3BO_5 (Tables SM1, SM2 of Supplementary Materials [30]) were used. For Co_3BO_5 the high symmetry of $Co4O_6$ octahedral environment (the smallest component of the electric field gradient $V_{zz} = -0.28\ e/Å^3$) was found that is in agreement with the low spin state of Co^{3+} ions occupying this site.

3. Results

3.1. The group-theoretical analysis

In this section we perform a group-theoretical analysis to classify the experimentally observed magnetic structures, described in Section 1.

In Fe_3BO_5 the iron magnetic moments in the triad 4-2-4 are antiferromagnetically (↑↓↑) or ferromagnetically ordered (↑↑↑) along the triad, with antiferromagnetic chains along the c-axis, after Ref. [4] and [15], respectively. In the 3-1-3 triads, the magnetic order is antiferromagnetic (↑↓↑), leading to the antiferromagnetically coupled ferromagnetic chains running along c-axis, with magnetic moments being aligned along the a-axis, as reported in both Refs. [4] and [15]. Therefore, in all cases the magnetic moment ordering is antiferromagnetic along the c axis, and each triad has just one magnetic component. As we show below, the magnetic ordering in the triads 4-2-4 and 3-1-3 is associated with a variety of irreducible representations τ6 and τ7 (τ3), respectively, at $k = 0$ case (Table 1, Tables SM3–SM5 [30]). In these irreducible representations the magnetic moment can have two components in triad 4-2-4, and three components in triad 3-1-3.

In terms of the Fe_3BO_5 low-temperature phase with space group *Pbnm* (62) the iron ions in triad 4-2-4 occupy three different symmetry 4c positions (4c1, 4c2 and 4c3, respectively). Each of these positions, whose moment transforms as the irrep τ6, is occupied by just one component, as said above, thus fixing the moments at the equivalent sites in the cell unit. However, there are three possible collinear orientations of the iron ions magnetic moments in the triad 4-2-4, since they are not related by symmetry, namely ↑↓↑, ↑↑↑ and ↑↑↓. In all cases, the magnetic moments ordering along the c axis is antiferromagnetic and the total magnetic moment is zero. The two first options correspond to the experimental neutron diffraction data [4] and [15], respectively. The third option involves the emergence of spin dimers in the triad 4-2-4 ↑↑↓ with ferromagnetic related magnetic moments Fe4-Fe2. This type of the magnetic ordering is in agreement with the results of theoretical studies [19] where the dimeric complexes were reviewed and the bevel angle of the magnetic moments in Fe4b position has been determined.

Table 1
The basis vectors of irreducible representations $\tau3$, $\tau6$, and $\tau7$ for Fe_3BO_5 (Pbnm (62)).

Position	Basis vectors	
3-1-3 spin ladder		
	$\tau7$	$\tau3$
4a	(x,y,z), (x,y,−z), (x,−y,−z), (x,−y,z)	(x,y,z), (x,y,−z), (−x,y,z), (−x,y,−z)
8d	(x,y,z), (x,y,z), (x,y,−z), (x,y,−z), (x,−y,−z), (x,−y,−z), (x,−y,z), (x,−y,z)	(x,y,z), (x,y,z), (x,y,−z), (x,y,−z), (−x,y,z), (−x,y,z), (−x,y,−z), (−x,y,−z)
4-2-4 spin ladder		
	$\tau6$	
4c1	(x,y,0), (−x,−y,0), (x,−y,0), (−x,y,0)	
4c2	”	
4c3	”	

The ordering in 3-1-3 triads deserves an individual discussion. The Fe_3BO_5 unit cell contains two spin ladders 3-1-3 and 3′-1′-3′, propagating along the c axis. According to the group-theoretical analysis, it can be distinguished that two possible orientations of the magnetic moments in the ladders transform as the irreducible representations τ7 and τ3. In both cases, the magnetic moments in the triads 3-1-3 will be oriented antiferromagnetically, and the triad's ordering along the c axis is ferromagnetic. However, according to the τ7 irreducible representation, the magnetic moments in both ladders 3-1-3 and 3′-1′-3′ are similarly oriented (↑↓↑) and (↑↓↑), while according to the irreducible representation τ3, moments in 3-1-3 (↑↓↑) and 3′-1′-3′ (↓↑↓) are oppositely directed. In case of $\tau7$ the total magnetic moment per unit cell is not completely cancelled (2 μ_B/f.u.), resulting in a ferrimagnetic (Ferri) ground state, while the antiferromagnetic ground state (AF) with zero magnetic moment per unit cell is expected according to the $\tau3$ (Table 1).

For the $k = 0$ case of Co_3BO_5 (space group *Pbnm* 55) there are eight irreducible representations τ1–τ8 (Table SM4), among which only four τ1, τ3, τ5 and τ7 correspond to the magnetic ordering on all ions. For τ1 and τ7 irreducible representations the ordering is antiferromagnetic and ferromagnetic (ferrimagnetic), respectively, with only c-axis component of the magnetic moment. For τ3 and τ5 the magnetic moment has a- and b-axis components with antiferromagnetic and ferromagnetic (ferri) ordering for different components. The τ5 has been reported as the best reproducing the experimental NPD data [22].

3.2. Superexchange interactions

In the ludwigite structure, depending on the M-O-M bond angle, different types of exchange paths can be distinguished: 77–100°, which are considered as 90° superexchange ($J1$, $J3$–$J7$, $J9$, and $J11$), and 115°, 118°, 162° superexchange interactions ($J2$, $J8$ and $J10$, respectively). The geometrical parameters associated with these paths are summarized in Table SM6 [30] and are shown in Fig. 2. The magnetic ions belonging to the same crystallographic positions are coupled via two common oxygen atoms (edge-sharing) forming magnetic chains 1-1, 2-2, 3-3, 4-4 propagated along c-axis (the superexchange interactions $J1$, $J4$, $J7$, and $J11$, respectively). Within the 3-1-3 spin ladder the magnetic chains are linked via a common oxygen atom (corner-shared FeO_6 octahedra) to form a square spin lattice ($J2$). Thus, for 3-1-3 spin ladder the superexchange paths take place via the side of the square in the absence of diagonal bonds (Fig. 2(a)). Within the 4-2-4 spin ladder the magnetic ions 2 and 4 have two superexchange paths: the first is via two common oxygen atoms ($J6$) and the second is the diagonal bond M-O-M with bond angle of 162° ($J10$) (Fig. 2(b)). The interaction between the ladders is described by exchange integrals $J3$, $J5$, $J8$, and $J9$ (Fig. 2(c)). As a result, the superexchange interactions in ludwigites can be adequately described by exchange integrals $J\lambda$ (λ ranges from 1 to 11). The obtained composition and number of exchange bonds are characteristic for ludwigites with any atomic composition. The expressions for $J\lambda$ generally depend on the types of interacting ions, possible ways of interaction, taking into account the symmetry, and the type of the individual d-orbitals. These expressions obtained for Fe_3BO_5 are listed in Table SM7. The absolute values of calculated superexchange interaction integrals are shown in Figure SM1 [30] for iron ludwigite as an example. The results clearly show that the most intense contribution to the magnetic state of a given system is made by the antiferromagnetic

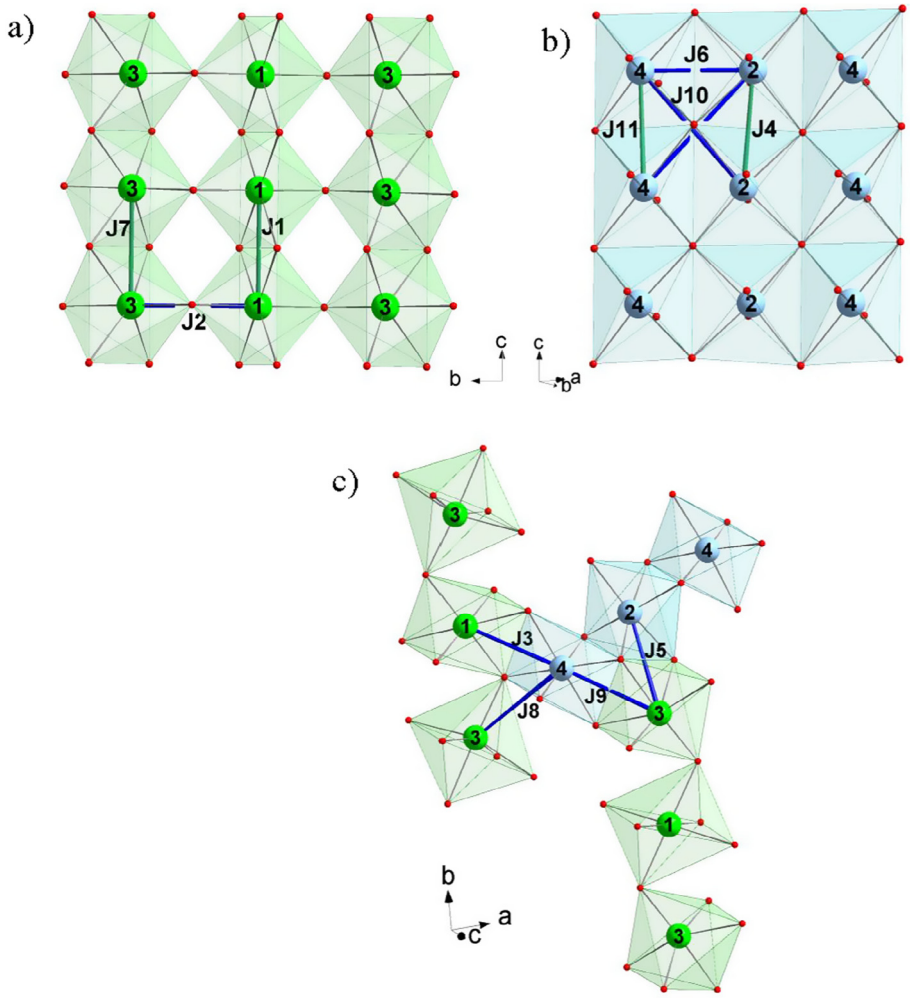

Fig. 2. The intra-ladders superexchange interactions 3-1-3 (a), 4–2-4 (b) and inter-ladders superexchange interactions (c). The intra-chain and inter-chain interactions are highlighted in green and blue, respectively. (For interpretation of the references to colour in this figure legend, the reader is referred to the web version of this article.)

interactions ($J\lambda < 0$). The strongest ones are a 90° exchange interactions with Fe^{3+} ions in site 4 ($J3$, $J9$, and $J11$) and the interaction between Fe^{2+} ions in positions 2 and 3 ($J5$). Medium in value are the negative interactions $J2$, $J6$, $J8$, and $J10$, which are the result of the FM and AF contributions competition as well as due to the specific spatial arrangement of cations with an angle different from 90°.

The comparison of the exchange integrals values for Fe_3BO_5 and Co_3BO_5 are shown in Table 2. The superexchange interactions parameters for Co_3BO_5 were taken from the Reference [21], where a wrong value in $J5$ was found and is now corrected to +1.88 K. It should be noted that for both compounds the superexchange interactions between M^{2+} ions located in the sites 1, 2 and 3 ($J1$, $J4$ and $J7$, respectively) are positive indicating the tendency to form ferromagnetic chains 1-1, 2-2, 3-3 along the c-axis, while a negative interaction between the M^{3+} ions belonging to the site 4 ($J11$) reflects a trend to the antiferromagnetic arrangement. Following the arguments in Section 3.1, we consider below the possible collinear spin configurations in the homometallic ludwigites which satisfy the mentioned irreducible representations in that section.

Table 2
The superexchange integrals $J\lambda$(K) in homometallic ludwigites. z is the number of nearest neighbours.

$J\lambda$	Interacting pair	z	Fe_3BO_5	Co_3BO_5	Belong to triad
$J1$	1-1	2	+1.16	+3.50	3-1-3
$J2$	1-3	2	−2.64	−2.89	3-1-3
$J3$	1-4	4	−5.38	−4.50	
$J4$	2-2	2	+1.16	+3.50	4-2-4
$J5$	2-3	4	−5.70	+1.88	
$J6$	2-4	2	−2.29	−1.97	4-2-4
$J7$	3-3	2	+1.16	+3.50	3-1-3
$J8$	3-4	2	−2.58	−6.64	
$J9$	3-4	2	−5.54	−2.44	
$J10$	2-4	4	−3.58	−4.23	4-2-4
$J11$	4-4	2	−5.29	−5.45	4-2-4

To find the magnetic ground state of the Fe_3BO_5 system, we have considered various magnetic configurations possible within the supercell. Of these, we have selected six configurations, including the overall magnetic ground state of the system. These configurations are labelled as S1–S6. The ferromagnetic (F, ↑↑↑), antiferromagnetic (AF, ↑↓↑) and dimer (D, ↑↑↓) alignments of Fe moments within the 4-2-4 triad and antiferromagnetic order along the c-axis are considered. Both F and AF spin alignments within the 3-1-3 triad and ferromagnetic order along c-axis are taking into account.

In the framework of the mean field theory the calculated total energies of all these configurations using general form

$$E = -\frac{1}{2}\sum_{ij} J_{ij}\boldsymbol{S}_i\boldsymbol{S}_j \tag{2}$$

where $\boldsymbol{S}_i$, $\boldsymbol{S}_j$ are spins of interacting ions, J_{ij} is superexchange interaction

Table 3
The possible collinear spin configurations and their calculated energies ΔE[a] for Fe_3BO_5. The magnetic moments direction along *c*-axis is shown for each spin ladder.

	3–1-3	4–2-4	ΔE, meV
S1	↑↓↑ ↑↓↑	↑↑↑ ↓↓↓	0.00
S2	↑↑↑ ↑↑↑	↑↑↑ ↓↓↓	8.89
S3	↑↓↑ ↑↓↑	↑↓↑ ↓↑↓	14.56
S4	↑↑↑ ↑↑↑	↑↓↑ ↓↑↓	23.46
S5	↑↓↑ ↑↓↑	↑↓↓ ↑↑↓	50.05
S6	↑↑↑ ↑↑↑	↑↓↓ ↑↑↓	64.62

[a] Relative to the energy of ferromagnetic state *S*1.

integral, are summarized in Table 3.

Note, that the conditions for frustration, namely the presence of triangular arrangements of magnetic moments, and interactions of opposite signs acting on one moment are present in all considered structures. However, among the ferromagnetic (F), antiferromagnetic (AF) and dimer (D) spin configurations; the F (S1) is found to have the lowest energy, thus it may be considered to be the most probable magnetic ground state of the system, where Fe moments in triad 4-2-4 are ferromagnetically aligned. We have estimated the energy difference between different magnetic states relative to this energy $\Delta E_i = E(Si) - E(S1)$. The AF configurations (*S*3) are ~14.6 meV higher in energy than the F, indicating that the former may represent a *meta*-stable state. The collinear dimer phase (*S*5) has a significant higher total energy. The ferromagnetic arrangement (↑↑↑) inside the 3-1-3 triad introduces additional frustrations of exchange interactions due to $J2 < 0$, thereby raising the system's energy (*S*2, *S*4, *S*6 for each F, AF and D configurations, respectively).

There are twelve possible collinear magnetic structures of Co_3BO_5 (C1–C12) appearing in accordance with group-theoretical analysis (Table 4). We have considered both ferromagnetic (C1–C7) and antiferromagnetic (C8–C12) orderings between the different types of spin ladders (3-1-3 and 3′-1′-3′) and (4-2-4 and 4′-2′-4′). The C1–C7 spin configurations are ferro- or ferrimagnetic structure corresponding to the different components of irreducible representations τ3(x), τ5(y) and τ7(z). The C8–C12 are antiferromagnetic spin structures corresponding to the different components of representations τ1(z), τ3(y) and τ5(x).

Table 4
The possible collinear spin configurations and their calculated energies ΔE[a] for Co_3BO_5. The magnetic moments are ordered ferromagnetically along the *c*-axis for both types of spin ladders.

	3-1-3	3′-1′-3′	4-2-4	4′-2′-4′	ΔE, meV (Co^{3+}, HS)	ΔE, meV (Co^{3+}, LS)
	Magnetic ordering corresponding to τ3(x), τ5(y),τ7(z)					
C1	↑↑↑	↑↑↑	↑↑↑	↑↑↑	0	0
C2	↑↓↑	↑↓↑	↑↑↑	↑↑↑	−3.7	−4.6
C3	↑↑↑	↑↑↑	↑↓↑	↑↓↑	3.7	5.8
C4	↓↑↓	↓↑↓	↑↑↑	↑↑↑	−16.8	1.3
C5	↑↑↑	↑↑↑	↓↑↓	↓↑↓	−58.3	0
C6	↑↓↑	↑↓↑	↑↓↑	↑↓↑	−19.4	1.3
C7	↑↓↑	↑↓↑	↓↑↓	↓↑↓	−44.19	−4.6
	Magnetic ordering corresponding to τ1(z), τ3(y),τ5(x)					
C8	↑↑↑	↓↓↓	↓↓↓	↑↑↑	−2.2	5.8
C9	↑↓↑	↓↑↓	↓↑↓	↑↓↑	−52.7	−4.6
C10	↑↓↑	↓↑↓	↑↓↑	↓↑↓	−10.9	1.3
C11	↓↓↓	↑↑↑	↑↓↑	↓↑↓	−29.6	0
C12	↑↑↑	↓↓↓	↑↓↑	↓↑↓	−25.0	5.8

[a] Relative to the energy of ferromagnetic state C1.

We have calculated the energies of the possible collinear magnetic structures for the cases of Co^{3+} high-spin (HS, S = 2) and low-spin state (LS, S = 0), using the superexchange interaction parameters from Table 2. As can be seen, the C5 spin configuration has the lowest energy, resulting in the most probable magnetic ground state of Co_3BO_5 system if both Co^{2+} (S = 3/2) and Co^{3+} (S = 2) ions are in high spin state. For a given spin configuration, all Co^{2+} magnetic moments in sites 1, 2, and 3 are ferromagnetically aligned and antiferromagnetically coupled with Co^{3+} magnetic moment in site 4. As a result, the magnetic moments ordering in the spin ladder 3-1-3 is ferromagnetic both along the triads (↑↑↑) and *c*-axis, while the magnetic moments in the spin ladder 4-2-4 have antiferromagnetic alignment (↓↑↓) along triad and ferromagnetic one along *c*-axis. The C2(C7) and C9 collinear spin structures were found to be most energetically favorable if Co^{2+} ions are in high-spin and Co^{3+} in low-spin configuration (S = 0). For C2(C7) spin structures the magnetic moments in the triads 3-1-3 are ordered antiferromagnetically, and the triad's ordering along the *c*-axis is ferromagnetic. The Co^{2+} magnetic moment at site 2 is antiferromagnetically aligned relative to those at site 1 and ferromagnetically relative to those at site 3. The C9 spin configuration differs only in that the two triads of each type are oriented oppositely. Note, that the C2(C7) spin configurations correspond to those experimentally found from the NPD study [22].

4. Discussion

4.1. Iron ludwigite

4.1.1. Antiferromagnetic arrangement in the triad 3-1-3 (↑↓↑)

In Fe_3BO_5, within the spin-ladder 3-1-3, the exchange interactions *J*1, *J*2 and *J*7 are all of ordering type, leading to the formation of the antiferromagnetically coupled ferromagnetic chains 1-1 and 3-3, extended along the *c*-axis. No frustration of exchange interactions is present in a given square spin lattice. The resulting collinear spin configuration within the 3-1-3 spin ladder satisfies the requirement of a local minimum of the exchange energy and coincides with that experimentally found from the neutron diffraction measurements [4,15].

4.1.2. Ferromagnetic arrangement in the triad 4-2-4 (↑↑↑)

Within the 4-2-4 spin ladder the negative exchange interaction *J*11 requires a division of the crystallographic positions 4*c* into six magnetic sublattices (2*a*, 2*d*, 4*a*, 4*b*, 4*c*, 4*d*) (see Table SM8.S1 [30]). The shortest inter-ionic distance 2.61 Å corresponds to the ion pair Fe^{2+}-Fe^{3+} located in the 2a–4a and 2d–4d positions. Taking the nearest-neighbours number $z = 2$, the strongly interacting spin exchange path is given by the antiferromagnetic spin chains 4a–4c, 4b–4d ($2J11 = -10.58$ K). This is accompanied by the doubling of the magnetic cell along the *c*-axis. In the 4-2-4 spin ladder all FeO_6 octahedra are linked via edge-sharing atoms leading to the additional nearest-neighbour diagonal superexchange path ($2J10 = -7.16$ K) with the bond angle of θ = 162°. The joint action of these two superexchange interactions determines the ferromagnetic spin arrangement within the triad 4-2-4 and antiferromagnetic arrangement along *c*-axis. In Fe_3BO_5 relatively weak positive intra-chain interaction Fe2-Fe2 (*J*4) and negative inter-chain interactions Fe2-Fe4 (*J*6) are frustrated. The so obtained most favorable spin arrangement corresponds to the S1 configuration in agreement with experiments by Bordet et al. [15].

4.1.3. Antiferromagnetic arrangement in the triad 4-2-4 (↑↓↑)

The inter-chain SE interaction Fe2-Fe4 *J*6 imposes antiferromagnetic arrangement along the 4-2-4 triad, while the diagonal Fe2-Fe4 exchange interaction *J*10 favors the ferromagnetic spin arrangement within the triad. The competition between these AF interactions results in the antiferromagnetic spin configuration S3 bringing about the frustration of exchange interactions *J*4 and *J*10. Negative intra-chain exchange interaction Fe4-Fe4 (*J*11) supports

antiferromagnetic order along *c*-axis, forming antiferromagnetically coupled antiferromagnetic chains. Such spin configuration has been proposed by Attfield et al. in the experimental work [4]. The ordering superexchange couplings (i.e. supporting the given spin structure) and frustrating ones are listed in the Table SM8.S3 [30].

4.1.4. Dimer arrangement in the triad 4-2-4 (↑↑↓)

The S5 spin configuration with the ferromagnetic order in the dimers Fe4a-Fe2a (Fe4d-Fe2d) is worth of attention. The magnetic moment of the third ion Fe4b (Fe4c) is antiparallel to the dimers magnetic moment (Table SM8.S5 [30]). The ferromagnetic dimers (*J*6 is frustrated bond) form a zigzag two-leg ladder along the *c*-axis. The antiferromagnetic coupling between dimers along the *c*-axis is clearly able to satisfy the strong diagonal coupling *J*10 but not the antiferromagnetic couplings *J*10 and *J*11 between the single iron ion Fe4b (Fe4c) and dimer Fe4a-Fe2a (Fe4d-Fe2d). As a result, the spin configuration is characterized by huge frustrations of superexchange interactions. Such spin configuration is unstable and in the presence of more strong interactions, e.g. from the spin ladder 3-1-3 (*J*3, *J*8, and *J*9), the Fe4b and Fe4c spin canting relative to the magnetic moment of the Fe4-Fe2 dimer can arise. Such non-collinear spin configuration was previously considered in the framework of density functional approach where the rotation of ~80° of the Fe^{3+} spin relative to the dimers spin was found [19]. Both for the AF (↑↓↑) and D (↑↑↓) spin configurations the frustration of the exchange interactions is significantly enlarged in comparison with F (↑↑↑) spin configuration as can be seen from graphical presentations shown in a last column of Table SM8.

The next physically important result is that for all considered collinear spin configurations, which were built in accordance to irreducible representations τ7(τ3) and τ6, the ordered (supporting the long-range order) and disordered (frustrated) magnetic couplings between the 3-1-3 and 4-2-4 ladders are equal in magnitude and compensate each other. Indeed, the geometrical spin frustrations in ludwigites stem from the topological features of the crystal structure where the 3D net of superexchange interaction between the spin ladders via M1 (*J*3) and M3 (*J*5, *J*8, and *J*9) ions are formed by triangles (Fig. 3). In Fe_3BO_5 all of these interactions are antiferromagnetic. For such a system, one cannot construct a ground state with all bonds fully satisfied. The ground state is degenerate and does not correspond to the minimum of the interaction energy of every spin pair. The impossibility

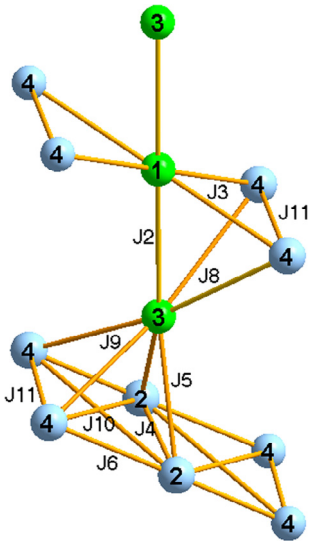

Fig. 3. Superexchange interactions between the 3-1-3 and 4-2-4 spin ladders in ludwigite structure. The 2D triangle spin lattice built by M1 and M4 ions is potentially frustrated if all bonds are antiferromagnetic. The magnetic ion M3 is being at the top of two polyhedra. In Fe_3BO_5, where *J*5, *J*8, and *J*9 bonds are all negative, it results in 3D frustrated magnetic structure.

to minimize the energy on all magnetic bonds leads to the heavy frustrations between the ladders in Fe_3BO_5.

In the presence of such massive magnetic frustrations, the long-range order should set on at low temperatures or be completely suppressed. However, one observes relatively high temperature long range ordering, thus frustration effects are actually quenched. One way to envisage such quenching is by considering that the magnetic system can be separated into two subsystems with orthogonal spin arrangement. The absence of frustrations in the orthogonal spin arrangement leads to the decoupling in the magnetic subsystems experimentally observed in Fe_3BO_5. Each of the subsystems has relatively high critical temperature (T_{N1} = 110, T_{N2} = 74 K). One can suppose that such unusual magnetic structure is favoured by magneto-crystalline anisotropy and Dzyaloshinskii-Moriya interactions.

4.2. Cobalt ludwigite

As can be seen from Table 2 the FM contribution to superexchange interactions increases in Co_3BO_5 resulting in the increase in positive intra-chain interactions 1-1, 2-2, and 3-3 ($J1 = J4 = J7 = +1.16$ for Fe_3BO_5 and +3.5 K for Co_3BO_5) and the decrease in the negative inter-chain ones *J*3, *J*6, *J*9. The main effect is the change in sign of the superexchange interaction between magnetic ions Co2 and Co3 ($J5 = -5.7$ K for Fe_3BO_5 and +1.88 K for Co_3BO_5). If all cobalt ions are in the high-spin state (C5 spin configuration) then strong negative inter-ladder (*J*8, *J*9) and intra-ladder (*J*6, *J*10) superexchange interactions determine the magnetic order in the system. These interactions along with the positive intra-chain interactions *J*1, *J*4, and *J*7 form the ferromagnetically coupled ferromagnetic chains in 3-1-3 spin ladder and the antiferromagnetically coupled ferromagnetic chains in the 4-2-4 spin ladder propagated along *c*-axis. The interactions Co1-Co3 (*J*2) and Co4-Co4 (*J*11) are superexchange interactions inside the spin ladders, which are not able to satisfy the given spin configuration. At the same time, no frustration of exchange interactions is present between the spin-ladders (Table SM9.C5).

It is interesting, that if Co^{3+} ion in site 4 is nonmagnetic (low-spin state) then for all spin structures (C2(C7) and C9) there are no frustrations of superexchange interactions (Table SM9.C2(C7)). Indeed, all interactions including the negative become of the ordering type. As result, the spin ordering within the 3-1-3 spin ladder is antiferromagnetic along the triad (↑↓↑) and ferromagnetic along the *c*-axis. These triads are ferromagnetically coupled with each other via Co2. The resulting collinear spin configuration coincides with that experimentally found [22]. The main conclusion is that the frustrations of the superexchange interactions existing in Co_3BO_5 system for high-spin state of Co^{3+} ion are quenched for the low-spin state, causing the long-range order.

4.3. Comparison with magnetization experiments

In our previous work [14] the methodology of rotating sample magnetometry around the *c*-axis has been applied to Fe_3BO_5 and Co_3BO_5 single crystals. It is convenient to remember in the discussion that in the case of Fe_3BO_5 if the magnetic field is applied along *a*-axis the hysteresis cycle opens at T_{N2} as expected for a ferrimagnetic order of Fe3 and Fe1 sublattices. However, the coercive field increases and the remanent magnetization decreases with decreasing temperature (Fig. 4a). At $T = 30$ K the M_r and coercivity become zero, indicating that the system transforms to antiferromagnetic phase (AFM2) (inset to Fig. 4a). The remanent magnetization M_r (T_{N2}) = 0.16 μ_B/f.u. is in stark discrepancy with the value of M_r = 2.36 μ_B/f.u. deduced from the NPD data [15]. The results of our group-theoretical analysis can help to resolve this issue. According to the magnetic representation τ3, the adjacent spin ladders 3-1-3 and 3′-1′-3′ are antiferromagnetically coupled resulting in zero magnetic moment per unit cell. The small value of the experimental magnetic moment M_r shows that in the temperature range

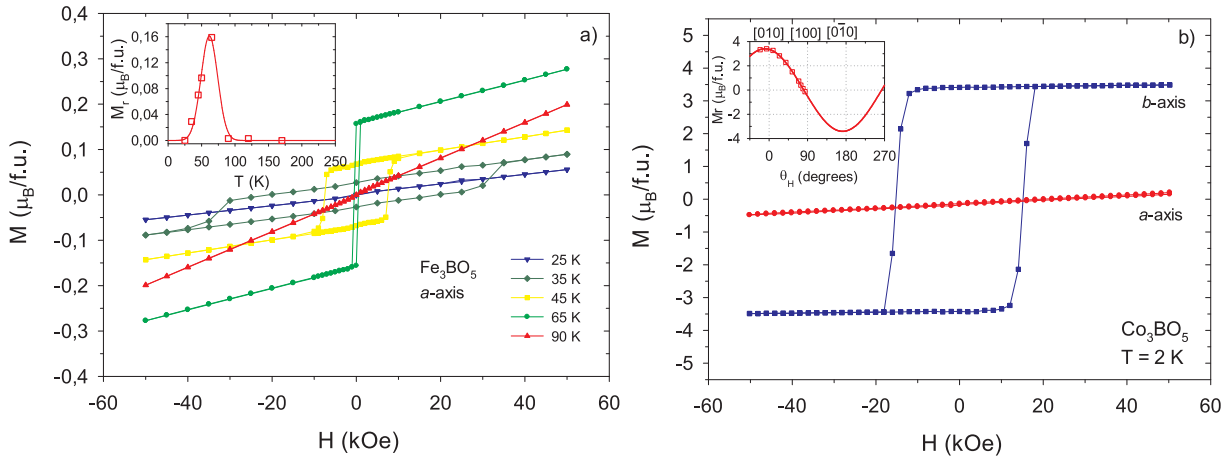

Fig. 4. a) Hysteresis cycles of Fe_3BO_5 single crystal as a function of the temperature with H applied along a-axis. Inset: the remanent magnetization M_r as a function of the temperature. b) Hysteresis cycles of Co_3BO_5 single crystal at $T = 2$ K, H applied along the b and a axes. The inset shows the variation of remanent magnetization M_r as a function of rotation around the c axis (θ_H).

of $30 < T < T_{N2}$ there is a slight tilt of the resulting magnetic moments of 3-1-3 and 3′-1′-3′ spin ladders. Below T = 30 K these magnetic moments are ordered antiferromagnetically resulting in zero remanent magnetic moment per unit cell. In our view, the ground-state in Fe_3BO_5 is antiferromagnetic (AFM2), and comprises two virtually independent orthogonal subsystems.

At the orthogonal arrangement of 3-1-3 and 4-2-4 spin ladders, the magnetic coupling between the 3-1-3 and 3′-1′-3′ ladders is effective, and consequently long-range order can set on due to other weak interactions, such as the Dzyaloshinskii-Moriya interactions or the super-superexchange interactions M-O-B-O-M (J_{SSE}) with bond length determined by the inter-ionic distance O-O in BO_3 group (2.39–2.41 Å) (Fig. 5). Recent studies of $BiCoO_3$ [31], $A_2Cu(PO_4)_2$ (A = Ba, Sr) [32], $RMnO_3$ (R = La, Pr, Nd) [33] have shown that SSE interactions are important for understanding the dimensionality of magnetic properties. The strength of an M-O-···-O-M spin exchange is primarily governed by the O-···-O distance and the ∠M-O-···-O angles and becomes negligible when the O-···-O contact is longer than the van-der-Waals distance (i.e., 2.8 Å). The potentially weak SSE can gain importance at low temperatures and in the presence of competing SE interactions.

The high anisotropy with easy magnetization axis (b-axis) is the main characteristic of Co_3BO_5 [14]. If an external field is applied along the b-axis, the hysteresis cycle is open, with the remanent magnetization $M_r = 3.4(1)\ \mu_B$/f.u. or $\sim 1.1\ \mu_B$/Co (Fig. 4b). The remanent magnetization M_r as a function of angle rotation around the c-axis (θ_H) is shown in the inset to Fig. 4b. As the angle between the applied field and b-axis increases the coercive field increases and the hysteresis cycle is transformed into a linear dependence, with M_r decreasing down to zero. This indicates the antiferromagnetic arrangement of the cobalt magnetic moments along the a-axis. The value of M_r obtained from magnetic measurements is in good agreement with that of $1.4\ \mu_B$/Co deduced from the NPD [22].

For Co_3BO_5 there are three possible spin configurations as mentioned above. The assumption that all cobalt ions are in the high-spin state (C5 spin configuration) gives the residual magnetic moment of $2\ \mu_B$/f.u. that is much less than that observed. For C2(C7) and C9 spin configurations (the low-spin state of Co4 ions) the residual magnetic moments equal $3\ \mu_B$/f.u. and $0\ \mu_B$/f.u., respectively. The former value is in good agreement with experiment. Thus, we conclude that the magnetic ground state of Co_3BO_5 is ferrimagnetic corresponding to C2(C7) spin configuration with magnetic moments oriented along the b-axis.

The magnetic bc-planes formed by the spin ladders 3-1-3 mediated by Co2 ions are spatially separated along the a-axis by BO_3 groups and nonmagnetic Co4 ions. The weakness of magnetic coupling via site 4 actually leads to the dimensional transition from 3D to quasi 2D. In this

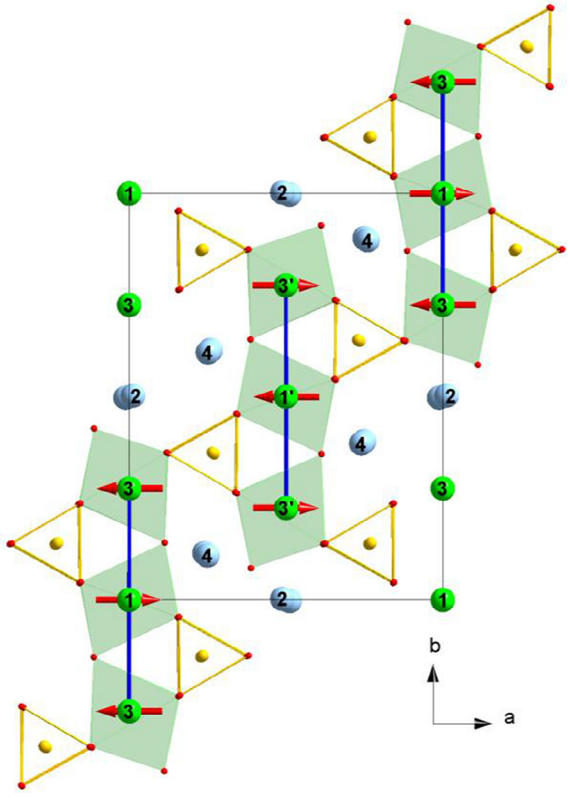

Fig. 5. The super-superexchange interactions between two types of ladders 3-1-3 and 3′-1′-3′ in the Fe_3BO_5 unit cell. The triangles denote BO_3 groups. Magnetic moment directions are according to the irreducible representations $\tau 3$ with zero magnetic moment per unit cell.

case the super-superexchange interactions of Co^{2+}-O–B–O–Co^{2+} can contribute to the onset of long-range order. The super-superexchange interaction Co^{2+}-O-Co^{3+}-O-Co^{2+} between two Co^{2+} ions in the neighbour bc –planes via the e_g-orbitals of the intermediate low spin Co^{3+} ion appears only in the fourth order perturbation theory $J_{SSE} \sim t^4/U^3$ and is much weaker than the standard Anderson contribution for two neighbour spins $J_{SE} \sim t^2/U$, where t is the effective cation-cation hopping via intermediate oxygen orbitals and U is the intraatomic Coulomb interaction for Co d-electrons.

5. Conclusion

We have performed a theoretical study of the Fe_3BO_5 and Co_3BO_5 magnetic structures by combining the symmetry and empirical approaches. The group-theory analysis has shown that the Fe_3BO_5 magnetic structure is described within two different magnetic representations for magnetic subsystems 3-1-3 ($\tau 7$ ($\tau 3$)) and 4-2-4 ($\tau 6$). The different collinear spin structures including ferromagnetic, antiferromagnetic and dimer arrangements in the 4-2-4 triad were considered. The ferromagnetic spin configuration was found to have lowest total energy among the considered ones and to correspond to neutron diffraction data [15]. An enhancement of the ferromagnetic contribution to superexchange interactions was found in Co_3BO_5 as compared to Fe_3BO_5.

We have shown the underlying role of the magnetic frustrations in the ludwigites. In Fe_3BO_5 the antiferromagnetic superexchange interactions between two spin ladders are highly frustrated due to triangle arrangement of iron ions. To reduce their effect, an orthogonal arrangement of the magnetic ordering in two magnetic subsystems takes place, leading to the experimentally observed decoupling of these subsystems. The long-range order within each subsystem sets on at a relatively high critical temperature. The small value of the residual magnetic moment arises from antiferromagnetic coupling between adjacent 3-1-3 and 3′-1′-3′ spin ladders in accordance with the irreducible representation $\tau 3$.

For Co_3BO_5 we have considered two cases of spin state for Co^{3+} and have found that the frustrations of exchange interactions exist when Co^{3+} ions are in the high spin state, and disappear when Co^{3+} ions are in the low spin state.

The obtained results well explain experimental magnetic data for Fe_3BO_5 and Co_3BO_5 and provide new understanding of the physics of frustrated ludwigites.

Acknowledgments

The Russian Foundation for Basic Research, Russia (project no. 17-02-00826-a). S.G.O. thanks the Russian Academy of Science, Russia (project no. 0356-2017-0030) for financial support. J.B. and A.A. acknowledge the financial support of the Spanish MINECO-MAT2017-83468R project, Aragonese E-12 17R RASMIA (co-funded by Fondo Social Europeo), and the European Union (FEDER (ES)).

Appendix A. Supplementary data

Supplementary data to this article can be found online at https://doi.org/10.1016/j.jmmm.2018.10.126.

References

[1] L. Balents, Spin liquids in frustrated magnets, Nature 464 (2010) 199–208.
[2] A.P. Ramirez, A. Hayashi, R.J. Cava, R. Siddharthan, B.S. Shastry, Nature 399 (1999) 333–335.
[3] J.E. Greedan, Geometrically frustrated magnetic materials, J. Mater. Chem. 11 (2001) 37–53.
[4] J.P. Attfield, J.F. Clarke, D.A. Perkins, Physica B Condens. Matt. 180 (1992) 581–584.
[5] J.C. Fernandes, R.B. Guimaraes, M. Mir, M.A. Continentino, H.A. Borges, G. Cernicchiaro, E.M. Baggio-Saitovitch, Phys. B Condens. Matt. 281 (2000) 694–695.
[6] M. Mir, R.B. Guimaraes, J.C. Fernandes, M.A. Continentino, A.C. Doriguetto, Y.P. Mascarenhas, L. Ghivelder, Phys. Rev. Lett. 87 (14) (2001) 147201.
[7] R.B. Guimarães, M. Mir, J.C. Fernandes, M.A. Continentino, H.A. Borges, G. Cernicchiaro, E. Baggio-Saitovitch, Phys. Rev. B 60 (9) (1999) 6617.
[8] J. Larrea, D.R. Sánchez, F.J. Litterst, E.M. Baggio-Saitovitch, J.C. Fernandes, R.B. Guimarães, M.A. Continentino, Phys. Rev. B 70 (17) (2004) 174452.
[9] D.C. Freitas, R.B. Guimaraes, D.R. Sanchez, J.C. Fernandes, M.A. Continentino, J. Ellena, G.G. Eslava, Phys. Rev. B 81 (2) (2010) 024432.
[10] D.C. Freitas, M.A. Continentino, R.B. Guimaraes, J.C. Fernandes, J. Ellena, L. Ghivelder, Phys. Rev. B 77 (18) (2008) 184422.
[11] G.A. Petrakovskiĭ, L.N. Bezmaternykh, D.A. Velikanov, A.M. Vorotynov, O.A. Bayukov, M. Schneider, Phys. Solid State 51 (10) (2009) 2077–2083.
[12] E. Moshkina, S. Sofronova, A. Veligzhanin, M. Molokeev, I. Nazarenko, E. Eremin, L. Bezmaternykh, J. Magnet. Magn. Mater. 402 (2016) 69–75.
[13] N.B. Ivanova, A.D. Vasilyev, D.A. Velikanov, N.V. Kazak, S.G. Ovchinnikov, G.A. Petrakovskii, V. Rudenko, Phys. Solid State 49 (2007) 651.
[14] J. Bartolomé, A. Arauzo, N.V. Kazak, N.B. Ivanova, S.G. Ovchinnikov, Y.V. Knyazev, I.S. Lyubutin, Phys. Rev. B 83 (14) (2011) 144426.
[15] P. Bordet, E. Suard, Phys. Rev. B 79 (14) (2009) 144408.
[16] M.H. Whangbo, H.J. Koo, J. Dumas, M.A. Continentino, Inorgan. Chem. 41 (8) (2002) 2193–2201.
[17] M. Matos, J. Solid State Chem. 177 (12) (2004) 4605.
[18] E. Vallejo, M. Avignon, Phys. Rev. Lett. 97 (21) (2006) 217203.
[19] M. Matos, J. Terra, D.E. Ellis, A.S. Pimentel, J. Magn. Magn. Mater. 374 (2015) 148–152.
[20] M. Matos, arXiv:1009.5899 [cond-mat.mtrl-sci].
[21] N.V. Kazak, N.B. Ivanova, O.A. Bayukov, S.G. Ovchinnikov, A.D. Vasiliev, V.V. Rudenko, J. Bartolome, A. Arauzo, Y.V. Knyazev, J. Magn. Magn Mater. 323 (5) (2011) 521–527.
[22] D.C. Freitas, C.P.C. Medrano, D.R. Sanchez, M.N. Regueiro, J.A. Rodríguez-Velamazán, M.A. Continentino, Phys. Rev. B 94 (17) (2016) 174409.
[23] P.W. Anderson, Phys. Rev. 115 (1) (1959) 2.
[24] G.A. Sawatzky, W. Geertsma, C. Haas, J. Magn. Magn. Mater. 3 (1–2) (1976) 37–45.
[25] M.V. Eremin, Phys. Solid State 24 (2) (1982) 423.
[26] O.A. Bayukov, A.F. Savitskii, Phys. Status Solidi B 155 (1989) 249.
[27] J.B. Goodenough, Phys. Rev. 100 (2) (1955) 564.
[28] J. Kanamori, J. Phys. Chem. Solids 10 (2–3) (1959) 87–98.
[29] P.W. Anderson, Phys. Rev. 79 (2) (1950) 350.
[30] Supplemental Material for “Effect of magnetic frustrations on magnetism of the Fe_3BO_5 and Co_3BO_5 ludwigites”.
[31] T. Sudayama, Y. Wakisaka, T. Mizokawa, H. Wadati, G.A. Sawatzky, D.G. Hawthorn, T.Z. Regier, K. Oka, M. Azuma, Y. Shimakawa, Phys. Rev. B 83 (23) (2011) 235105.
[32] H.-J. Koo, D. Dai, M.-H. Whangbo, Inorgan. Chem. 44 (12) (2005) 4359–4365.
[33] T. Kimura, S. Ishihara, H. Shintani, T. Arima, K.T. Takahashi, K. Ishizaka, Y. Tokura, Phys. Rev. B 68 (6) (2003) 060403.